A&A 481, 319–326 (2008)
DOI: 10.1051/0004-6361:20078050
© ESO 2008

Astronomy & Astrophysics

Spectroscopy and multiband photometry of the afterglow of intermediate duration γ-ray burst GRB 040924 and its host galaxy

K. Wiersema[1], A. J. van der Horst[1], D. A. Kann[2], E. Rol[3], R. L. C. Starling[3,1], P. A. Curran[1], J. Gorosabel[4], A. J. Levan[5], J. P. U. Fynbo[6], A. de Ugarte Postigo[4], R. A. M. J. Wijers[1], A. J. Castro-Tirado[4], S. S. Guziy[4], A. Hornstrup[7], J. Hjorth[6], M. Jelínek[4], B. L. Jensen[6], M. Kidger[8], F. Martín-Luis[9], N. R. Tanvir[3], P. Tristram[10], and P. M. Vreeswijk[11]

[1] Astronomical Institute "Anton Pannekoek", University of Amsterdam, Kruislaan 403, 1098 SJ Amsterdam, The Netherlands
e-mail: kwrsema@science.uva.nl
[2] Thüringer Landessternwarte Tautenburg, Sternwarte 5, 07778 Tautenburg, Germany
[3] Department of Physics and Astronomy, University of Leicester, University Road, Leicester, LE1 7RH, UK
[4] Instituto de Astrofísica de Andalucía (IAA-CSIC), Apartado de Correos, 3004, 18080 Granada, Spain
[5] Department of Physics, University of Warwick, Coventry, CV4 7AL, UK
[6] Dark Cosmology Centre, Niels Bohr Institute, University of Copenhagen, Juliane Maries Vej 30, 2100 Copenhagen, Denmark
[7] Danish National Space Center, Juliane Maries Vej 30, Copenhagen 0, 2100, Denmark
[8] ESA-European Space Astronomy Centre, Villafranca del Castillo, PO Box 50727, 28080 Madrid, Spain
[9] Instituto de Astrofísica de Canarias, C/. Via Lactea s/n, 38205 La Laguna, Tenerife, Spain
[10] University of Canterbury, Private Bag 4800 Christchurch 8140, New Zealand
[11] European Southern Observatory, Alonso de Córdova 3107, Casilla 19001, Santiago 19, Chile

Received 9 June 2007 / Accepted 14 December 2007

ABSTRACT

Aims. We present optical photometry and spectroscopy of the afterglow and host galaxy of gamma-ray burst GRB 040924. This GRB had a rather short duration of $T_{90} \sim 2.4$ s, and a well sampled optical afterglow light curve. We aim to use this dataset to find further evidence that this burst is consistent with a massive star core-collapse progenitor.

Methods. We combine the afterglow data reported here with those from the literature and compare the host properties with survey data.

Results. We find that the global behaviour of the optical afterglow is well fit by a broken power-law, with a break at ~0.03 days. We determine the redshift $z = 0.858 \pm 0.001$ from the detected emission lines in our spectrum. Using the spectrum and photometry we derive global properties of the host, showing it to have similar properties to other long GRB hosts. We detect the [Ne III] emission line in the spectrum, and compare the fluxes of this line of a sample of 15 long GRB host galaxies with survey data, showing the long GRB hosts to be comparable to local metal-poor emission line galaxies in their [Ne III] emission. We fit the supernova bump accompanying this burst, and find that it is similar to other long GRB supernova bumps, but fainter.

Conclusions. All properties of GRB 040924 (the associated supernova, the spectrum and SED of host and afterglow) are consistent with an origin in the core-collapse of a massive star.

Key words. gamma rays: bursts – galaxies: distances and redshifts – cosmology: observations

1. Introduction

The large sample of γ-ray bursts (GRBs) detected by the BATSE instrument on board the CGRO satellite clearly shows that GRBs can be classified in two distinct classes, based on spectral hardness and duration (Kouveliotou et al. 1993), though the possibility of three classes has also been proposed (e.g. Horváth et al. 2006; see also Hakkila et al. 2003). The difference in duration and spectral hardness may reflect important differences in the production mechanism of relativistic jets by the progenitor object, and therefore may be an important clue to the nature of the progenitor. The great difficulty in obtaining accurate γ-ray positions for the short-hard burst population made searches for afterglows unsuccessful for a long time. With the arrival of Swift and its ability to rapidly identify X-ray afterglows also for faint and short duration bursts, this situation changed dramatically, resulting in several localisations of short bursts by both Swift and HETE-2, and the detection of X-ray and optical afterglows for a considerable fraction of these (e.g. the review by Nakar 2007, and references therein).

With the different sensitivity and spectral range covered by these satellites with respect to BATSE, the classification of bursts into the classes of short and long burst became more ambiguous in several cases, for example due to long lasting soft tails detected in the prompt emission of bursts that BATSE would have classified as members of the short-hard class (e.g. Norris & Bonnell 2006 and references therein). The question of the progenitors of short bursts versus long bursts can now be approached through other angles, such as the presence of a supernova (SN), the nature of the host galaxies of a large sample of bursts, the density of the medium in which the afterglow propagates and its gradient, the circumburst environment through afterglow spectroscopy to name just a few (Lee & Ramirez-Ruiz 2007; Nakar 2007 and references therein). The distinction between short and long GRBs is however under strong debate. Classification only by the duration of the prompt emission has proved to be weak for identifying progenitor models (see also the

Table 1. Log of observations of GRB 040924 reported in this paper. We note that the last NOT exposure is close to the limiting magnitude.

Δt (d)	Magnitude, Error (1σ)	Band / frequency	Telescope	Exp. time	Seeing
0.204	21.3 ± 0.5	*R*	MOA	4 × 5 m	1.8
0.568	Upper limit 18.2 (3σ)	*H*	OSN MAGIC	85 × 30 s	1.2
0.666	22.97 ± 0.09	*V*	VLT FORS2	3 × 3 m	0.6
0.674	22.56 ± 0.13	*R*	VLT FORS2	3 × 2 m	0.6
0.679	21.95 ± 0.19	*I*	VLT FORS2	3 × 2 m	0.6
0.731	22.59 ± 0.15	*R*	NOT ALFOSC	9 × 15 m	1.5
0.871	23.27 ± 0.08	*V*	VLT FORS2	3 × 3 m	0.9
0.878	22.85 ± 0.13	*R*	VLT FORS2	3 × 2 m	0.9
0.890	22.08 ± 0.19	*I*	VLT FORS2	3 × 2 m	0.9
2.97	23.38 ± 0.29	*R*	NOT ALFOSC	5 × 10 m	1.2
28.64	23.3 ± 0.2	*I*	WHT Aux	4 × 15 m	1.3
28.69	24.1 ± 0.30	*R*	WHT Aux	4 × 15 m	1.7
31.72	Upper limit 19.8 (3σ)	K'	CAHA Omega2000	92 × 30 s	1.8
32.58	Upper limit 19.6 (3σ)	K'	CAHA Omega2000	213 × 30 s	1.6
108.39	23.6 ± 0.2	*I*	WHT Aux	4 × 15 m	1.2
295.69	24.39 ± 0.30	*R*	WHT Aux	3 × 15 m	0.9
0.663	Flux < 96 μJy (3σ)	4.9 GHz (6 cm)	WSRT	12 h	
5.541	Flux < 81 μJy (3σ)	4.9 GHz (6 cm)	WSRT	12 h	
32.48	Flux < 75 μJy (3σ)	4.9 GHz (6 cm)	WSRT	12 h	
	Flux < 63 μJy (3σ)	4.9 GHz (6 cm)	WSRT combined data	36 h	

recent detection of two long bursts without supernovae, Fynbo et al. 2006a; Gal-Yam et al. 2006; Della Valle et al. 2006; Gehrels et al. 2006). A large sample of datasets covering prompt emission, afterglow and host galaxies of GRBs at both sides of the classical 2-s limit is required. In this paper we focus on the properties of GRB 040924. This burst has a duration very close to the classical 2-s long-short divide, and has been considered a short burst candidate (e.g. Fan et al. 2005).

GRB 040924 was localised by the Fregate and WXM instruments onboard the HETE-2 satellite on 2004 September 24 at 11:52:11 UT (Fenimore et al. 2004), and also detected by satellites within the IPN network (Golenetskii et al. 2004). The burst was classified as an X-ray rich burst, based on the ratio of the fluences of the burst in the 7–30 keV and the 30–400 keV bands. Donaghy et al. (2006) report a T_{90} duration of 2.39 ± 0.24 s from the HETE-2 data, and show that the duration alone would make this burst a good candidate for membership of the short GRB class. However, a clear spectral lag is present and the spectrum is soft, favouring a long burst class membership (Donaghy et al. 2006). As such it is an interesting burst to study.

In this paper we present our dataset on the afterglow and host GRB 040924, supplemented with observations from literature. In Sect. 2 we describe our observations. In Sect. 3 we analyze the afterglow data, and in Sect. 4 the data on the host galaxy. In Sect. 5 we derive general properties for the associated supernova in relation to other GRB related supernovae, and in Sect. 6 we present our conclusions and discussion.

2. Observations and analysis

2.1. Afterglow optical photometry

Due to the quick localisation by HETE-2, the Palomar 60 inch telescope was able to rapidly find a candidate for the optical afterglow associated with this burst (Fox & Moon 2004; Soderberg et al. 2006). We observed the afterglow of GRB 040924 at several different observatories. All data were reduced with standard IRAF and MIDAS packages. Cosmic ray hits were removed using the L.A.Cosmic software by Van Dokkum (2001). Astrometric calibration was done using the USNO-B1.0 catalogue. Photometry was done using the IRAF DAOPHOT and APPHOT packages. The *V*, *R* and *I* band images were calibrated relative to the photometric sequence provided by Henden (2004). The log of photometric observations and their results are shown in Table 1.

We imaged the error box with the 0.6 m telescope at Mt. John Observatory (+ MOA camera) in the wide *R*-band filter. A 300-s single image was obtained through clouds at 0.087 days after burst, but did not detect the afterglow. Further imaging at 0.2 days marginally detected the afterglow. Two epochs of *V*, *R* and *I* band imaging of the afterglow position were made with the Very Large Telescope (VLT) in Cerro Paranal (Chile), using the Focal Reducer – Low Dispersion Spectrograph (FORS2) on UT1 (Antu). The conditions during the first epoch were excellent (seeing ~0.6 arcsec), but seeing increased in the second epoch. Two afterglow observations were made with the 2.56-m Nordic Optical Telescope (NOT) at La Palma. Observations were carried out using the Andalucía Faint Object Spectrograph and Camera (ALFOSC). We performed an *H*-band observation using the near-infrared MPI für Astronomie General-Purpose Infrared Camera (MAGIC) on the 1.5 m telescope at Observatorio de Sierra Nevada, which we calibrated using 2MASS field stars.

2.2. Host galaxy spectroscopy

Attempts at measuring the redshift from afterglow spectroscopy using the William Herschel Telescope (WHT) on La Palma on September 25 and 26 unfortunately proved unsuccessful due to bad weather decreasing the signal to noise ratio. Therefore we obtained a dark time spectrum aimed at obtaining the host galaxy redshift using VLT UT1 (Antu) with the FORS2 instrument in long slit spectroscopy (LSS) mode on October 10, approximately 15.75 days after burst. A bright star marked as *G* in Fig. 1 was used to position the slit, 27 arcsec away from the host galaxy; the position angle was approximately 25.1 degrees. Two spectra of 1800 s exposure time each were taken, using the 300V and 300I grisms, to increase wavelength coverage. We used a 1 arcsec slit. Both exposures were performed without an order sorting filter to increase sensitivity, so the red end of the 300V is contaminated by the second order (which has twice the resolution and wavelength). As there are no lines

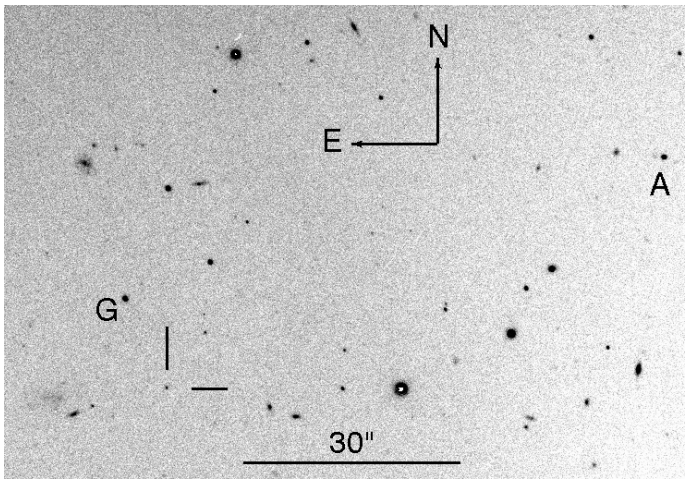

Fig. 1. Cut from the first epoch VLT FORS2 *I* band observation, showing the afterglow marked by tickmarks. The star marked by *G* was used to align the FORS2 slit for the host galaxy spectroscopy. The moving object marked by *A* is a main belt asteroid which was present in the first epoch *V*, *R* and *I* band observations.

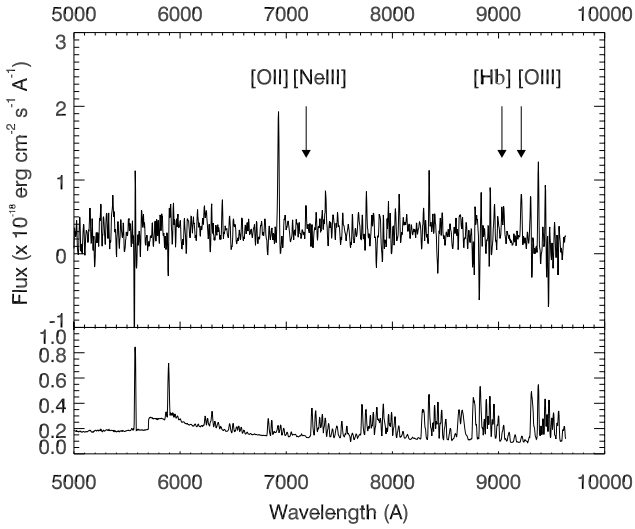

Fig. 2. The averaged VLT FORS2 300V and 300I spectrum of the host galaxy (*upper panel*), with corresponding error spectrum (*lower panel*). The prominent [O II] line is labelled. The spectrum is smoothed by 3 pixels for displaying purposes.

visible in the bluest region and the continuum is undetected, this has no influence on the measured emission line fluxes. Both spectra have been reduced in a standard fashion using the data reduction package IRAF. The L.A.Cosmic program (specifically the *lacos_spec* routine) written by Van Dokkum (2001) was used to remove both point- and irregular shaped cosmic ray hits from the science and standard images. The wavelength resolution is estimated by measuring the FWHM of the arc lines at 10.2 Å for the 300V, and 9.6 Å for the 300I spectrum. The spectra were flux calibrated using the standard star LTT1788 (Hamuy et al. 1992; 1994). Atmospheric extinction correction was made by applying a mean extinction curve for Paranal. A Galactic extinction correction was performed by using the $E(B-V)$ value of 0.058 mag (Schlegel et al. 1998), assuming a Galactic extinction law A_λ/A_V expressed as $R_V = A_V/E(B-V)$ (Cardelli et al. 1989). We make the standard assumption $R_V = 3.1$ (Rieke & Lebofsky 1985).

The combined spectra and the associated error spectrum are shown in Fig. 2. The continuum level of the host galaxy is faint, with a mean signal to noise ratio of ~2 per pixel. We find several emission lines in the spectra, which we present in Table 2. All of these lines are consistent with a redshift $z = 0.858 \pm 0.001$. No other faint, galaxy-like sources, visible in the WHT imaging data near the GRB host galaxy, fell in the slit.

2.3. Radio observations

The radio observations reported in this paper are all made using the Westerbork Synthesis Radio Telescope (WSRT) in the Netherlands. Three observations at the position of the afterglow were made, all at 4.9 GHz. Data reduction was performed using the MIRIAD software (Sault et al. 1995). No significant detection of an afterglow was found in any of the three epochs, see Table 1. To search for a radio host galaxy, we combined the data of all three observations. Again no radio source is found on the position of the afterglow, with corresponding 3σ upper limit of 63 μJy. A formal flux measurement for a point source at the location of the optical afterglow gives a value of 12 ± 21 μJy for the combined data.

Table 2. Spectroscopy results for the 300V and 300I grism. We list conservative 1σ uncertainties for the line fluxes. For lines that were detected in both grism spectra, a weighted average of the fluxes was used. Spectra are corrected for Galactic extinction.

Line ID	Line flux $\times 10^{-17}$ erg s^{-1} cm^{-2}	Wavelength (Å)	Redshift
[O II] λ3727.4	2.31 ± 0.14	6927.3	0.858
[Ne III] λ3868.8	0.47 ± 0.17	7187.7	0.858
Hβ λ4861.3	0.44 ± 0.20	9031.7	0.858
[O III] λ4958.9	0.94 ± 0.24	9214.8	0.858

2.4. Supernova search and host galaxy

The observations reported in this section were aimed at observing a possible supernova associated with GRB 040924, which was later identified through much deeper HST imaging (Soderberg et al. 2006). A redshifted, K-corrected extrapolation of supernova 1998bw would yield expected *SN* magnitudes of $R \sim 24.6$ and $I \sim 23.8$ (Sect. 5) making it possible for us to detect it with ground based telescopes. Observations were made with the Auxiliary Port Imaging Camera (Aux-Port Imager) mounted at the auxiliary port of the Cassegrain A&G box of the William Herschel Telescope (WHT). The first epoch was made on October 23, consisting of 4×15 min in *I* and 4×15 min in *R*. Whilst at the start of observations the conditions were good, the seeing greatly deteriorated during the exposures, which, combined with an increasing airmass, led to a relatively shallow limiting magnitude and low image quality of the combined *R* band exposure.

A second epoch of *I* band imaging was performed on January 10, aimed at observing the host galaxy. The observations were done in the same manner as the first epoch, consisting of 4×15 min exposure time. The host galaxy is clearly detected. A second epoch of *R* band imaging was performed on July 16 2005, consisting of 3×15 min.

To obtain a broadband colour estimate of a potential supernova, two K' band observations were made near the supernova peak with the Omega2000 near-infrared wide field camera on the prime focus of the 3.5 m telescope at the Calar Alto

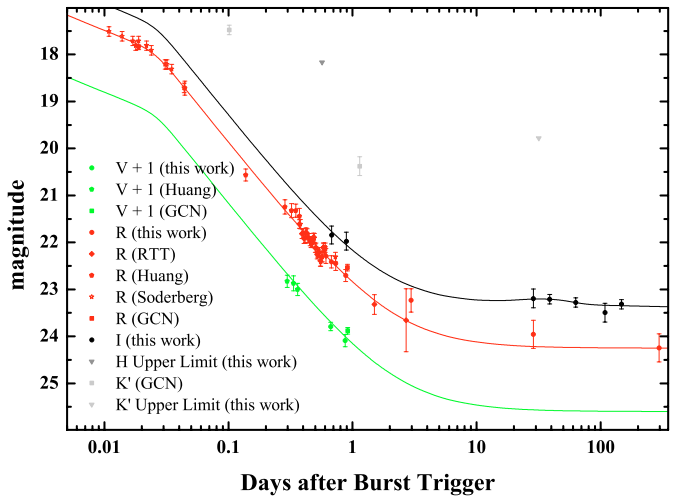

Fig. 3. Light curves of the afterglow of GRB 040924, fitted with an achromatic broken power-law. The top curve is the I band lightcurve and the middle curve is R band. The lower curve shows the V band curve where 1 mag is added for clarity. Data are from this paper and sources given in Sect. 3. The I band fit includes the contribution of a supernova.

observatory, on 2004 October 26 and 27, with exposure times 2760 and 6390 s respectively. The host and SN are not detected.

We note here that the photometric calibration of the WHT data are hampered by the very small field of view (the Aux Port imager has a circular field of view of 1.8 arcmin diameter, but dithering required for fringe correction reduced the useful field of view to approx 1.2 arcmin). No Henden (2004) calibration stars can be used to calibrate the R band data, as there are only two of these in the field of view, and they are saturated. We use the NOT data to calibrate field objects, however most objects near the GRB host which are in both NOT and WHT R band data are galaxies. The I band WHT data provided a better calibration due to the fact that more unsaturated Henden stars were present in the WHT I band image due to slightly different pointing and dithering. We therefore point out that particularly the R band magnitudes of the WHT data should be treated with caution.

3. The afterglow

We gathered published data from the literature (Terada et al. 2004a,b; Silvey et al. 2004; Huang et al. 2005; Soderberg et al. 2006) and combined these with our data, also adding data from the RTT 150 telescope (I. Khamitov, priv. comm.[1]; Khamitov et al. 2004). We corrected the afterglow magnitudes for Galactic extinction where needed. The resulting light curve is shown in Fig. 3.

We used the fitting method described in Curran et al. (2007) which fits the data from all available bands simultaneously, assuming that each band has the same power-law decay but leaving free the offset between bands to account for differences in filter curves and calibration. We refer to Curran et al. (2007) for details on the fitting method and error analysis. Our fit using all available data shows a broken power-law, with values of the afterglow decay index of $\alpha_1 \sim 0.31$, $\alpha_2 = 1.25 \pm 0.02$ and a break time of ~0.03 days, where the break smoothness is fixed at a value $s = 10$, with a best fit $\chi^2/\mathrm{dof} = 1.2$. We note that the pre-break decay (α_1) and the break time are not well constrained, the χ^2 is fairly insensitive to changes in these parameters. The R band afterglow shows a low significance wiggle around the best fit power-law, most noticeably around ~0.5 days. This is commonly seen in well sampled afterglow lightcurves, and does not affect our afterglow fit noticeably.

Using the data set presented in this paper, Kann et al. (2006) found that the $VRIK'$ spectral energy distribution (SED) of the afterglow of GRB 040924 is fit well by a power-law plus SMC-like extinction, though the data are also well fit with no extinction. The extinction-corrected spectral slope is $\beta = 0.63 \pm 0.48$ and the host galaxy extinction is $A_V = 0.16 \pm 0.44$, agreeing with the value of the spectral slope $\beta = 0.61 \pm 0.08$ reported by Silvey et al. (2004), who do not fit for extinction. A comparison with other intrinsic GRB afterglow luminosities (Kann et al. 2006) shows that the afterglow of GRB 040924 was the faintest in their sample of pre-Swift GRB afterglows with observed optical counterparts in multiple bands and enough sampling to derive temporal and spectral indices.

Soderberg et al. (2006) have previously noted the break from a shallow decay to a more common temporal decay index, and our decay slopes and break time agree with theirs, but improve on accuracy particularly for α_2. This break is not consistent with a jet break, as the difference in temporal decay index is not as expected from a jet break, the break being very early, and both pre- and post-break decay slopes being too shallow (cf. Zeh et al. 2006 for a large sample of optical afterglow parameters). Huang et al. (2005) reach similar results qualitatively, but have very different values due to a much smaller dataset. The early data showing this break have only been taken in R band so it is unclear whether this break is achromatic, but after the early break, multi-colour data are available. The case of the synchrotron cooling and peak frequency redward of the observed optical frequency after the break, i.e. $\nu_\mathrm{m} < \nu_\mathrm{c} < \nu_\mathrm{opt}$, is ruled out, as the spectral and temporal slope cannot be accomodated together in the standard blastwave model (e.g. Zhang & Mészáros 2004). The case for $\nu_\mathrm{m} < \nu_\mathrm{opt} < \nu_\mathrm{c}$ using a homogeneous density medium or a $1/r^2$ (stellar wind) medium would give $p \sim 2.7$ for a wind medium and $p \sim 2.1$ for a homogeneous medium from the temporal decay. The spectral slope gives $p \sim 2.2$ in this case. The distinction between the homogeneous and wind medium can be made by assuming $n(r) \propto r^{-k}$, and calculating k using β and α (we refer to Starling et al. 2007 for details). For the post-break values we find $k = 1.6^{+0.3}_{-0.5}$, which agrees with an interpretation of a $1/r^2$ wind medium in which the blastwave propagates, though the uncertainties are quite large.

The change in decay slope of $\Delta\alpha \sim 0.9$ rules out the possibility that the break is caused by the passage of the cooling break ν_c, for which $\Delta\alpha = 0.25$ would be expected. This shallow decay phase and break can possibly be attributed to energy injection, a mechanism frequently invoked to explain shallow decay phases in afterglows (e.g. Nousek et al. 2006; Pandey et al. 2006). Using a parametrization $E \propto t^q$ (Nousek et al. 2006), we find $q \sim 0.7$ in the case of a homogeneous medium, and $q \sim 1.1$ in the case of a wind medium.

4. The host galaxy

We detect several emission lines in the VLT FORS2 spectra of the host (see Fig. 2), though the detections are of low significance due to the faintness of the host. The analysis of the emission lines was done using the Starlink DIPSO spectral fitting package, using mainly the ELF (emission line fitting) routines, and compared with results using the IRAF splot package. The

[1] http://hea.iki.rssi.ru/~rodion/040924

results were in agreement within errors. We note that several of the emission lines (particularly the [O III]λ5007) are affected by skylines and show differing fluxes in the 300V and 300I spectra, caused by the relative success of skyline subtraction. We have not included these lines in further analysis. In the case where an emission line is found with similar flux in the 300I as well as in the 300V spectrum, the average value is given.

The emission lines found in our host galaxy spectra allow us to securely determine the redshift at $z = 0.858 \pm 0.001$. The widths of the emission lines appear not to be significantly broadened, but are consistent with the instrumental resolution, as is expected from spectroscopy of other host galaxies and the spectral resolution that was used.

The ratios of the measured fluxes [OIII]/Hβ and [OII]/Hβ compared to those from samples of AGN and normal galaxies (Kennicutt 1992) show that the host galaxy spectrum is likely not dominated by (non-thermal) AGN emission. We do not significantly detect the Hγ line, with an upper limit lower than the expected flux based on the flux of the Hβ line and case B recombination, so we are not able to derive Balmer decrement values, and apply no host galaxy reddening correction to the spectrum. This is consistent with the absence of apparent absorption affecting the afterglow SED.

4.1. Star formation rate

To estimate the star formation rate (*SFR*) we use the expression from Kennicutt (1998),

$$SFR_{[\mathrm{OII}]} = 1.4 \times 10^{-41} L_{[\mathrm{OII}]}\ M_\odot\,\mathrm{yr}^{-1},$$

where $L_{[\mathrm{OII}]} = 4\pi d_{\mathrm{l}}^2 f_{[\mathrm{OII}],\mathrm{obs}}$, with d_{l} the luminosity distance. Using cosmological parameters $H_0 = 70$ km s^{-1}/Mpc, $\Omega_{\mathrm{M}} = 0.3$ and $\Omega_\Lambda = 0.7$ ($d_{\mathrm{l}} = 5.47$ Gpc), we find $SFR_{[\mathrm{OII}]} = 1.15 \pm 0.08\ M_\odot\,\mathrm{yr}^{-1}$. The real uncertainty in the *SFR* is much larger: the $SFR_{[\mathrm{OII}]}$ has been calibrated on the Hα *SFR* through empirical methods, providing an additional uncertainty through the scatter in this relation; and the effects of dust obscuration are uncertain (but likely negligible; see Sects. 3 and 4). This estimate for the star formation is very typical of long GRB host galaxies (Christensen et al. 2004).

The radio continuum flux of a normal (i.e. non-AGN hosting) galaxy is formed by synchrotron emission of accelerated electrons in supernova remnants and by free-free emission from HII regions (Condon 1992). It is expected that the radio continuum flux is a particularly good tracer of the recent *SFR*, due to the short expected lifetime of the supernova remnants, which is $\lesssim 10^8$ yr. We use the method by Berger et al. (2003) to calculate an upper limit on the unobscured *SFR*. The three WSRT observations (see Table 1) combined give a 3σ upper limit to the radio continuum flux of the host galaxy of 63 μJy (see Sect. 2.3), and from this limit we find a 3σ upper limit on the unobscured star formation of 137 $M_\odot\,\mathrm{yr}^{-1}$ (using the prescription in Berger et al. 2003). This is a limit deeper than that obtained for most GRB host galaxies at similar redshift (Berger et al. 2003). We note that the conversion of radio luminosity to *SFR* fails in cases where there is an appreciable contribution to the radio flux from an AGN component, though no association of a GRB to an AGN harbouring host galaxy has been seen so far.

4.2. Metallicity

As the metallicity of the progenitor object plays a crucial role in our understanding of the evolutionary process leading to GRBs (e.g. Yoon & Langer 2005), it is vital to secure metallicity measurements for as many GRB host galaxies as possible. In cases where this is not possible due to redshift or signal to noise constraints, we may be able to at least ascertain the possibility that the host has significant subsolar metallicity. The difference in progenitor properties between short and long bursts may also be reflected in the distribution of parameters of the host galaxies of GRBs, such as their metallicity (however, see Levan et al. 2007).

Metallicities of GRB host galaxies are in general hard to determine: the average redshift of GRBs is high, and the hosts tend to be faint. For the high redshift sample a line of sight value for the metallicity towards (long) GRBs can be obtained by observing the hydrogen column through the Lyman line(s) and the columns of lines that are not easily depleted in dust (e.g. sulphur or zinc). This method regularly provides very accurate values of the columns of elements (e.g. Savaglio et al. 2003; Fynbo et al. 2006b; Price et al. 2007; Prochaska et al. 2007), but as the data are obtained over a line of sight and GRBs influence their environments profoundly, the metals and hydrogen are not necessarily co-located (e.g. Watson et al. 2007). High quality measurements of oxygen abundance using electron temperatures (T_{e}), determined through the [O III]λ4363 line, can generally only be obtained for the very lowest redshift subsample of GRB hosts, and have so far only been possible for four cases (Prochaska et al. 2004; Hammer et al. 2006; Wiersema et al. 2007).

For GRB hosts at higher redshift, this line is often too faint to detect in a reasonable exposure time (except in cases of very high ionization parameter), and secondary indicators of metallicity are required. Extensive studies have been performed to find metallicity diagnostics that depend solely on bright emission lines and on their calibration with T_{e}-derived measurements. Generally the requirements of a secondary metallicity indicator are that the lines that are used are bright; that the correlation (based on local galaxies) with T_{e}-determined metallicities has a low dispersion; that the line fluxes can preferably be obtained in a single spectrum (i.e. lines that are close together in wavelength) and that preferably both high and low ionisation lines are used so the ionization parameter can be found. One of the most frequently used metallicity diagnostics using the brightest lines is the R_{23} method (Pagel et al. 1979). This method gives a low and a high metallicity solution for a value of R_{23}. This degeneracy can be broken through other lines, which are often fainter and more difficult to detect, and the ionization parameter needed to obtain a good value through R_{23} can be hard to determine in the case of high redshift and low signal to noise data. In the case of the host of GRB 040924, the [O III]λ5007 is located right on a skyline, which makes it impossible to measure its flux. Instead we use a fixed ratio of [O III] λ5007 to λ4959 of 3 (Izotov et al. 2006) to estimate the [O III] λ5007 at $\sim 2.8 \times 10^{-17}$ erg s^{-1} cm^{-2}. We find $R_{23} \sim 13.8$ and using the Kewley & Dopita (2002) formulas we find that the host flux ratio is located near the connection of the low and high metallcity branches, having a metallicity $12 + \log(\mathrm{O/H}) \sim 8.5$, but is badly constrained due to the large uncertainty in R_{23}, which is dominated by the uncertainty in Hβ. It has been noted by several authors that the R_{23} can give results discrepant from direct (T_{e}) measurements, and several empirical calibrations have been offered (e.g. Nagao et al. 2006). We find a value $12 + \log(\mathrm{O/H}) \sim 8.1$ from the R_{23} value of the host of 040924 when using the Nagao et al. (2006) calibrations.

More accurate secondary methods (e.g. involving the N II and S II lines) cannot be used for this host, as the diagnostic lines are redshifted out of the spectral range.

4.3. [Ne III] in GRB hosts

GRB host galaxies can be found up to high redshift, and in several cases spectra of host galaxies with redshifts even higher than $z \sim 1$ have been obtained. At these redshifts, the bright Hα and [O III]λ5007, 4959 are shifted out of the (useful) range of (low resolution) optical spectra, making any secondary calibrator that requires these lines or an accurate correction for reddening impossible to use. It has been noted (e.g. Bloom et al. 1998; Bloom et al. 2001; Djorgovski et al. 2001) that the [Ne III]λ3869 line is frequently detected in GRB host spectra, and its strength can be used to infer the presence of very massive stars. The ionization potentials of [Ne III] and [O III] are very similar (41.1 eV and 35.1 eV), so we may expect to use [Ne III] lines as a substitute for [O III] lines when the redshift is too high. An added advantage is the fact that the [Ne III]λ3869 is close in wavelength to the [O II]λ3727 line, making uncertainties in the reddening correction less pronounced when using ratios of these blue lines.

Nagao et al. (2006) gathered spectroscopic data from several samples of local galaxies with a broad range of metallicities, to derive unbiased samples of line fluxes and metallicities, in order to calibrate commonly used secondary metallicity indicators. Their analysis shows that at a given metallicity the ionisation parameter has a low dispersion, and that it depends strongly on metallicity. Based on their sample of galaxies, Nagao et al. propose using the ratio of the [Ne III] and [O II] fluxes as metallicity estimators in the absence of other, brighter high ionisation lines such as [O III] due to high redshift. This relation is of particular importance to long GRB hosts, as their redshift distribution peaks at $z \sim 2.8$ (Jakobsson et al. 2006), long GRB hosts tend to have high ionisation parameters and because the range up to $z \sim 1$ is most suitable to compare with other deep galaxy surveys (Savaglio 2006 and references therein).

We compiled a list of GRB host galaxies with published fluxes of [O II] and [Ne III]: 970228 (Bloom et al. 2001), 970508 (Bloom et al. 1998), 970828 (Djorgovski et al. 2001), 980613 (Djorgovski et al. 2003), 990712 (Vreeswijk et al. 2001), 000418 (Bloom et al. 2003), 020405 (Price et al. 2003), 020903 (Hammer et al. 2006), 030329 (Gorosabel et al. 2005), 031203 (Prochaska et al. 2004), 040924 (this work), 050824 (Sollerman et al. 2007), 060218 (Wiersema et al. 2007), 060505 (GRB position, Thöne et al. 2007) and 060912A (Levan et al. 2007, priv. comm.). We compared the log ([Ne III]/O II]) values of these hosts with those of the SDSS (DR3) sample of galaxy spectra with T_e derived oxygen abundances of Izotov et al. (2006), i.e. a sample of emission line galaxies with detected [O III]λ4363. This line becomes undetectable when the metallicity increases above $12 + \log(\mathrm{O/H}) \sim 8.5$ (as the H II regions are too cool), so this is essentially a sample of metal-poor emission line galaxies. Figure 4 shows the resulting distributions. A Kolmogorov-Smirnov test shows that the GRB host sample is not significantly inconsistent (probability $P = 0.23$) with the SDSS sample of galaxies with T_e metallicity determinations. This result indicates that the sample of low redshift GRB host galaxies does not significantly differ from metal poor emission line galaxies as a whole in a similar redshift range in terms of the their integrated massive star populations, though the current GRB host spectroscopy sample is sparse and more data are required to be certain. The values of the host of GRB 980425 show that conclusions cannot be drawn about the site where the GRB occurred, but only on the integrated light of the galaxy, as has been shown in much more detail in Hammer et al. (2006) and Thöne et al. (2007). The value log ([Ne III]/[O II]) ~ -0.7 for the host of GRB 040924 is not an extreme value for a GRB host, and using the samples of Nagao et al. (2006) we find that the host has a metallicity of $12 + \log(\mathrm{O/H}) \sim 8.1$ from this flux ratio, matching the value from R_{23} (Sect. 4.2).

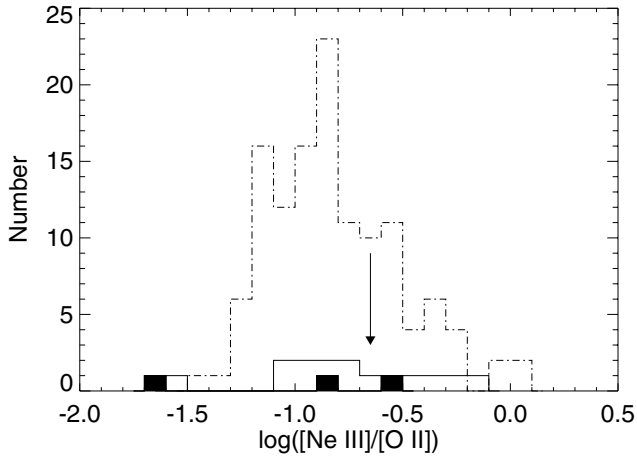

Fig. 4. Histogram showing the distributions of log ([Ne III]/[O II]): a dot-dashed line shows the SDSS spectrophotometric catalogue values of sources with a determined T_e metallicity from Izotov et al. (2006), 125 sources. The solid line shows the values for 14 GRB host galaxies (see text; 040924 noted with an arrow). In both cases we only use sources where both lines are detected. The filled squares show the values for the three regions in the host galaxy of GRB 980425 as determined by Hammer et al. (2006), where the highest value is the bright star-forming region where many WR stars are present, the middle value is taken at the GRB location, and the lowest at an H II region unrelated to the GRB (see Hammer et al. 2006 for details).

4.4. Host SED

The host galaxy of GRB 040924 is clearly detected in deep HST pointings (Soderberg et al. 2006; Wainwright et al. 2007). We use the detections in the *F775W* and *F850LP* filters, and add our *R* and *I* band detections from WHT, and upper limits in K' and *H* band from GCNs. The *R* band and HST bands straddle the 4000 Å break, and can therefore be used to determine some parameters of the host. We fit galaxy templates using the HyperZ program[2] developed by Bolzonella et al. (2000). We fit using the eight synthetic galaxy templates provided within HyperZ and using the spectroscopic redshift. We find that the host is best fit by a starburst template, and has $M_B \sim -18.7$, which confirms the HST results reported by Wainwright et al. (2007). The age of the stellar population is young (best fit ~0.12 Gyr) with little or no reddening, but these parameters are not well constrained as the *R* band magnitude is uncertain and bluer bands are not available, which makes the distinction between reddening and age hard to establish quantitatively. The best fit parameters are very similar to the sample of long GRB hosts analysed by Christensen et al. (2004). The absolute *B* band magnitude of the host and the estimated metallicity of $12 + \log(\mathrm{O/H}) \sim 8.1$ fits well in the local luminosity-metallicity relation (Salzer et al. 2005), though uncertainties are large. One characteristic of long GRB hosts is the relatively high specific *SFR* (Christensen et al. 2004). Assuming $M_B^* = -21.1$ and using the *SFR* from [O II], we find that the host of GRB 040924 has a SSFR $\sim 10\ M_\odot\ \mathrm{yr}^{-1}\ (L/L_*)^{-1}$. This value matches well with the range of SSFR ~5–12 found for a sample of 10 long GRB hosts analysed by Christensen et al. (2004).

[2] See http://webast.ast.obs-mip.fr/hyperz/

5. An associated supernova

We search for a supernova associated with GRB 040924 in the images from WHT (see Sect. 2.4) by searching for a bump in the late time light curve. Soderberg et al. (2006) use image subtraction with HST ACS data to derive the parameters of the supernova. They acquired three epochs, of which the first and third are in filters *F775W* and *F850LP*, and for the second epoch only *F775W* was used. Through image subtraction they find a rebrightening of the afterglow of more than a magnitude, a clear signal of a supernova bump.

We use the values reported in Soderberg et al. (2006) and Wainwright et al. (2007) for host and supernova measurements, and add to that our ground-based data from WHT and CAHA. We fit the full light curve of the afterglow + host galaxy + supernova using the method described in Zeh et al. (2004), using SN1998bw as the template supernova. As we only have good measurements of the SN bump in the I band, but the afterglow is determined well only in the R band, we use the R band afterglow as a reference light curve. The host galaxy magnitudes in I band determined from WHT and HST agree well with each other. We find a luminosity factor $k = 0.203 \pm 0.202$ and a stretch factor $s = 1.371 \pm 0.971$. Essentially, the SN bump is only marginally detected through this analysis. We take $k < 0.4$ (equivalent to a peak magnitude which is one magnitude fainter than SN 1998bw) as a conservative upper limit and thus confirm the finding of Soderberg et al. (2006) that the supernova associated with this burst is fainter than a K-corrected, redshifted SN 1998bw. This cannot be caused solely by extinction in the host: the analysis of the afterglow SED reveals a negligible amount of extinction along the line of sight. Even correcting for the possible small amount of extinction, this is still the faintest GRB-associated SN detected thus far (see Ferrero et al. 2006 and Sollerman et al. 2007 for the complete sample). It is most similar to the SN associated with GRB 970228 (Galama et al. 2000), but we caution that this SN was significantly brighter even without a correction for the extinction in the host galaxy. As the photometric calibration uncertainty adds a large amount to the WHT data uncertainties, we perform differential photometry with respect to bright field stars present in all WHT epochs, and find brightening with 2.2σ in I and 1.8σ in R, showing that while a SN 1998bw at this redshift would have easily been detected by WHT, a GRB-SN this much fainter requires higher signal to noise data.

6. Discussion and conclusions

It is clear that the standard differentiation between short and long bursts using solely their duration is not a clear enough way to also separate out the properties of their progenitors as a whole; the distributions of long and short bursts overlap significantly (Donaghy et al. 2006). The same goes for the properties of their host galaxies: there are clear associations of short GRBs with elliptical galaxies devoid of recent star formation (e.g. the case of GRB 050724, Berger et al. 2005), but there are also cases of actively star-forming, short burst host galaxies (e.g. Hjorth et al. 2005; Covino et al. 2005). The lack of an optical afterglow for many short bursts (and therefore a sub-arcsecond position) makes the association of a galaxy with a burst rather complicated (Levan et al. 2007), making the diagnostic power of a galaxy association less strong by selecting only the optically luminous cases. Possible progenitor models comprise several mechanisms (e.g. compact binary mergers, SGR giant flares), each contributing to the observed overall short burst population. A collection of parameters that can each on its own not decisively separate out different progenitor models, could in combination be used for population synthesis. In a sense these parameters are not much different from those which constrain long GRB progenitors. These include (but are not limited to): the luminosity function of both GRB and afterglow, requiring the redshift distribution and jet-break determinations; the age of the dominant stellar population, determined from host galaxy SED fitting; the quantity and age of the most massive stars, determined through WR signatures and high-excitation lines; the offset of GRBs from the hosts/star-forming regions; the abundance structure of the host galaxies, found through afterglow and emission line spectroscopy; the circumburst density and its structure, found from afterglow SED modelling; the jet opening angle distribution, etc. The sample of bursts which seem to find themselves close to the classic 2-s duration division are important in these studies, as they are likely to contain bursts from different progenitors and allow for easy comparison with the samples of long and short bursts.

GRB 040924 clearly finds its origin in the collapse of a massive star. The properties of the host galaxy fall within the range of the sample of long GRB host galaxies: the host is blue, is actively forming stars, and has significantly sub-solar metallicity. The afterglow, albeit faint with respect to other pre-Swift long GRBs, behaves similarly to other long GRBs. The supernova could have been missed if this burst had occured at significantly higher redshift. However, although there are short bursts which share one or two of the host/afterglow properties with this burst (see e.g. Prochaska et al. 2006 for an overview of short burst host properties such as metallicities, luminosities etc.), the combination of prompt emission, afterglow and host properties makes it clear that the progenitor was a collapsar. The part of prompt emission parameter space where both long and short bursts can be found (i.e. the part of the hardness – duration diagram where the two burst distributions overlap) is interesting to explore, as we may expect to find contributions from at least two progenitor scenarios.

Acknowledgements. We express our gratitude to ESO for granting our request for spectroscopy. We are very grateful to the observers who performed the observations reported here, and we thank particularly Ian Skillen for his assistance in the planning of GRB observations. We thank the anonymous referee for useful comments. We would like to thank Arne Henden for taking a deeper photometric calibration exposure. KW and PAC thank NWO for support under grant 639.043.302. This study is supported by Spanish research programmes ESP2002-04124-C03-01 and AYA2004-01515. This project is partly based on observations obtained at the ESO VLT under ESO programme 073.D-0465(B), PI R.A.M.J. Wijers. This paper is based on observations made with the William Herschel Telescope operated on the island of La Palma by the Isaac Newton Group in the Spanish Observatorio del Roque de los Muchachos of the Instituto de Astrofisica de Canarias; on observations made with the Nordic Optical Telescope, operated on the island of La Palma, jointly by Denmark, Finland, Iceland, Norway and Sweden, in the Spanish Observatorio del Roque de los Muchachos of the Instituto de Astrofísica de Canarias; and on observations collected at the German-Spanish Astronomical Center, Calar Alto, operated jointly by Max-Planck Institut für Astronomie and Instituto de Astrofísica de Andalucía (CSIC). The Westerbork Synthesis Radio Telescope is operated by ASTRON (Netherlands Foundation for Research in Astronomy) with support from the Netherlands Foundation for Scientific Research (NWO).

The authors acknowledge benefits from collaboration within the Research Training Network "Gamma-Ray Bursts: an enigma and a tool", funded by the EU under contract HPRN-CT-2002-00294.

References

Berger, E., Cowie, L. L., Kulkarni, S. R., et al. 2003, ApJ, 588, 99
Berger, E., Price, P. A., Cenko, S. B., et al. 2005, Nature, 438, 988
Bloom, J. S., Djorgovski, S. G., Kulkarni, S. R., et al. 1998, ApJ, 507, 25
Bloom, J. S., Djorgovski, S. G., & Kulkarni, S. R. 2001, ApJ, 554, 678

Bloom, J. S., Berger, E., Kulkarni, S. R., et al. 2003, AJ, 125, 999
Bolzonella, M., Miralles, J.-M., & Pello, R. 2000, A&A, 363, 476
Cardelli, J. A., Clayton, G. C., & Mathis, J. S. 1989, ApJ, 345, 245
Christensen, L., Hjorth, J., & Gorosabel, J. 2004, A&A, 425, 913
Condon, J. J. 1992, ARA&A, 30, 575
Covino, S., Malesani, D., Israel, G. L., et al. 2005, A&A, 447, 5
Curran, P. A., van der Horst, A. J., Beardmore, A. P., et al. 2007, A&A, 467, 1049
Della Valle, M., Chincarini, G., Panagia, N., et al. 2006, Nature, 444, 1050
Djorgovski, S. G., Frail, D. A., Kulkarni, S. R., et al. 2001, ApJ, 562, 654
Djorgovski, S. G., Bloom, J. S., & Kulkarni, S. R. 2003, ApJ, 591, 13
Donaghy, T. Q., Lamb, D. Q., Sakamoto, T., et al. 2006 [arXiv:astro-ph/0605570]
Fan, Y. Z., Zhang, B., Kobayashi, S., et al. 2005, ApJ, 628, 867
Fenimore, E. E., Ricker, G., Atteia, J.-L., et al. 2004, GCN Circ., 2735
Ferrero, P., Kann, D. A., Zeh, A., et al. 2006, A&A, 457, 857
Fox, D. B., & Moon, D.-S. 2004, GCN Circ., 2734
Fynbo, J. P. U., Watson, D., Thöne, C. C., et al. 2006a, Nature, 444, 1047
Fynbo, J. P. U., Starling, R. L. C., Ledoux, C., et al. 2006b, A&A, 451, 47
Galama, T. J., Tanvir, N., Vreeswijk, P. M., et al. 2000, ApJ, 536, 185
Gal-Yam, A., Fox, D. B., Price, P. A., et al. 2006, Nature, 444, 1053
Gehrels, N., Norris, J. P., Barthelmy, S. D., et al. 2006, Nature, 444, 1044
Golenetskii, S., Aptekar, R., & Mazets, E. 2004, GCN Circ., 2754
Gorosabel, J., Pérez-Ramírez, D., Sollerman, J., et al. 2005, A&A, 444, 711
Hakkila, J., Giblin, T. W., Roiger, R. J., et al. 2003, ApJ, 582, 320
Hammer, F., Flores, H., Schaerer, D., et al. 2006, A&A, 454, 103
Hamuy, M., Walker, A. R., Suntzeff, N. B., et al. 1992, PASP, 104, 533
Hamuy, M., Suntzeff, N. B., Heathcote, S. R., et al. 1994, PASP, 106, 566
Henden, A. A. 2004, GCN Circ., 2811
Hjorth, J., Watson, D., Fynbo, J. P. U., et al. 2005, Nature, 437, 859
Horváth, I., Balázs, L. G., Bagoly, Z., et al. 2006, A&A, 447, 23
Huang, K. Y., Urata, Y., Filippenko, A. V., et al. 2005, ApJ, 628, L93
Izotov, Y. I., Stasińska, G., Meynet, G., et al. 2006, A&A, 448, 955
Jakobsson, P., Levan, A., Fynbo, J. P. U., et al. 2006, A&A, 447, 897
Kann, D. A., Klose, S., & Zeh, A. 2006, ApJ, 641, 993
Kennicutt, R. C. 1992, ApJ, 388, 310
Kennicutt, R. C. 1998, ARA&A, 36, 189
Kewley, L. J., & Dopita, M. A. 2002, ApJS, 142, 35K
Khamitov, I., Aslan, Z., Yesilyaprak, C., et al. 2004, GCN Circ., 2749
Kouveliotou, C., Meegan, C. A., Fishman, G. J., et al. 1993, ApJ, 413, 101
Lee, W. H., & Ramirez-Ruiz, E. 2007, NJPh, 9, 17
Levan, A. J., Jakobsson, P., Hurkett, C., et al. 2007, MNRAS, 378, 1439
Nagao, T., Maiolino, R., & Marconi, A. 2006, A&A, 459, 85
Nakar, E. 2007, PhR, 442, 166
Norris, J. P., & Bonnell, J. T. 2006, ApJ, 643, 266
Nousek, J. A., Kouveliotou, C., Grupe, D., et al. 2006, ApJ, 642, 389
Pagel, B. E. J., Edmunds, M. G., Blackwell, D. E., et al. 1979, MNRAS, 189, 95
Pandey, S. B., Castro-Tirado, A. J., McBreen, S., et al. 2006, A&A, 460, 415
Price, P. A., Kulkarni, S. R., Berger, E., et al. 2003, ApJ, 589, 838
Price, P. A., Songaila, A., Cowie, L. L., et al. 2007, ApJ, 663, L57
Prochaska, J. X., Bloom, J. S., Chen, H., et al. 2004, ApJ, 611, 200
Prochaska, J. X., Chen, H.-W., Dessauges-Zavadsky, M., et al. 2007, ApJ, 666, 267
Rieke, G. H., & Lebofsky, M. J. 1985, ApJ, 288, 618
Salzer, J. J., Lee, J. C., Melbourne, J., et al. 2005, ApJ, 624, 661
Sault, R. J., Teuben, P. J., & Wright, M. C. H. 1995, Astronomical Data Analysis Software and Systems IV, ASP Conf. Ser., 77, 4, 433
Savaglio, S. 2006, NJPh, 8, 195
Savaglio, S., Fall, S. M., & Fiore, F. 2003, ApJ, 585, 638
Schlegel, D. J., Finkbeiner, D. P., & Davis, M. 1998, ApJ, 500, 525
Silvey, J., Allen, D., & Bayliss, M., et al. 2004, GCN Circ. 2833
Soderberg, A. M., Kulkarni, S. R., Price, P. A., et al. 2006, ApJ, 636, 391
Sollerman, J., Fynbo, J. P. U., Gorosabel, J., et al. 2007, A&A, 466, 839
Starling, R. L. C., van der Horst, A. J., Rol, E., et al. 2007, ApJ, in press [arXiv:0704.3718]
Terada, H., Akiyama, M., & Kawai, N. 2004a, GCN Circ., 2745
Terada, H., Akiyama, M., & Kawai, N. 2004b, GCN Circ., 2750
Thöne, C. C., Fynbo, J. P. U., Östlin, G., et al. 2007, ApJ, submitted [arXiv/astro-ph:0703407]
Van Dokkum, P. G. 2001, PASP, 113, 1420
Wainwright, C., Berger, E., & Penprase, B. E. 2007, ApJ, 657, 367
Watson, D., Hjorth, J., Fynbo, J. P. U., et al. 2007, ApJ, 660, 101
Wiersema, K., Savaglio, S., Vreeswijk, P. M., et al. 2007, A&A, 464, 529
Yoon, S.-C., & Langer, N., et al. 2005, A&A, 443, 643
Zeh, A., Klose, S., & Hartmann, D. H. 2004, ApJ, 609, 952
Zeh, A., Klose, S., & Kann, D. A. 2006, ApJ, 637, 889
Zhang, B., & Mészáros, P. 2004, IJMPA, 19, 2385